



Supplement of

Formation of highly absorptive secondary brown carbon through nighttime multiphase chemistry of biomass burning emissions

Ye Kuang et al.

Correspondence to: Ye Kuang (kuangye@jnu.edu.cn) and Shan Huang (shanhuang_eci@jnu.edu.cn)

The copyright of individual parts of the supplement might differ from the article licence.

1 **S1. Method of Aerosol liquid water content calculations**

2 The size resolved aerosol liquid water content (ALWC) was formulated as the following in which
3 the ALWC was the summation of aerosol water contributed by inorganic aerosols and organic aerosols:

4
$$ALWC(D_a)=ALWC_{Inorg}(D_a) + ALWC_{org}(D_a)$$

5 Where the $ALWC_{Inorg}(D_a)$ was calculated using the ISORROPIA (Kuang et al., 2018) model using
6 reverse mode and metastable with size resolved inorganic aerosol chemical compositions measured by
7 the SP-AMS as inputs. The $ALWC_{org}(D_a)$ was calculated as:

8
$$ALWC_{org}(D_a)=\frac{m_{org}(Da)}{\rho_{org}} \times \rho_w \times \frac{\kappa_{org}}{(\frac{100\%}{RH}-1)}$$

9 The $m_{org}(Da)$ is the size resolved organic aerosol mass concentrations measured by the SP-AMS,
10 the κ_{org} derived in Kuang et al. (2021) was used.

11

12

13

14

15

16

17

18

19

20

21

22

23

24

25

26

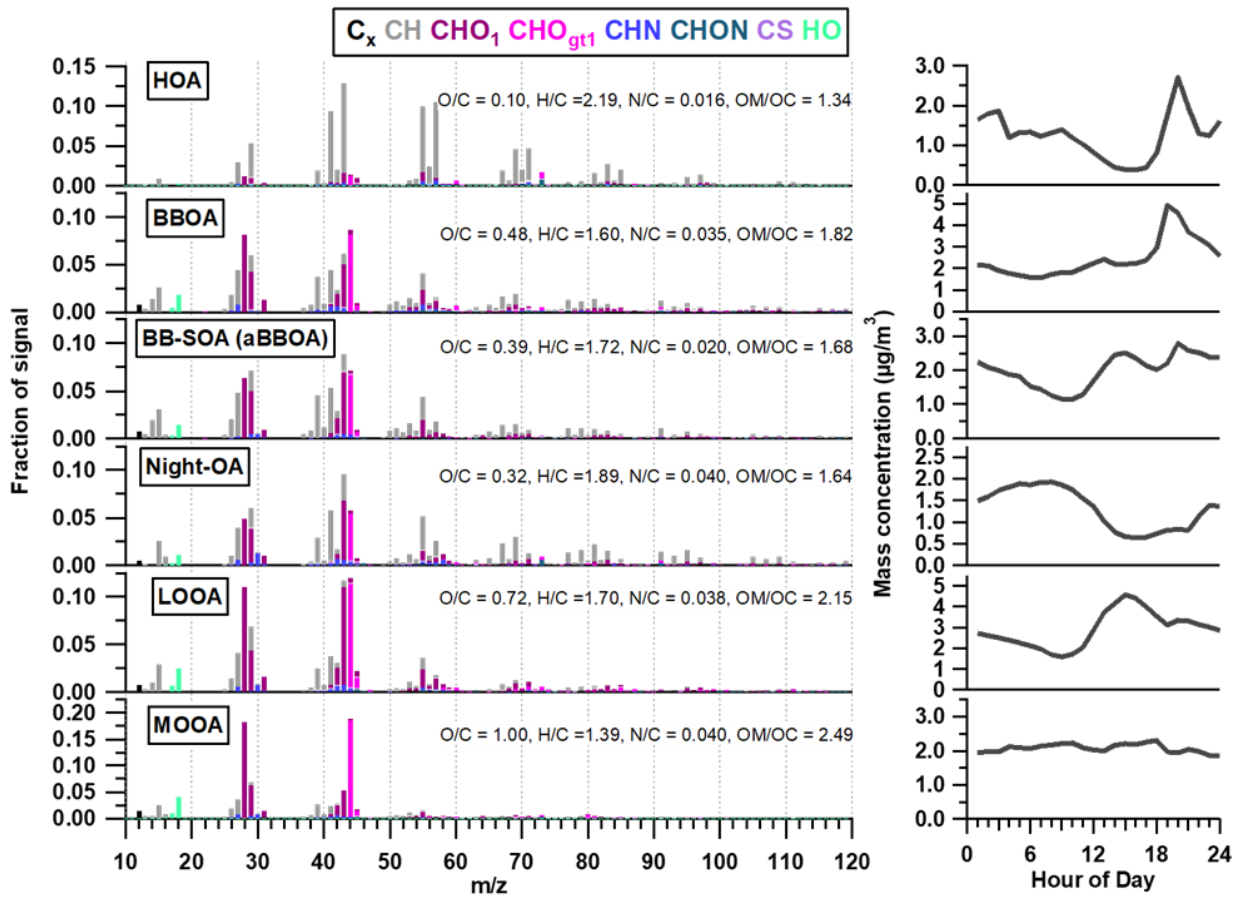
27

28

29

30 **S2. Supplementary Figures**

31
32
33
34



35
36
37
38
39
40
41
42
43
44
45
46
47
48
49
50
51

Figure S1. Mass spectral profile and diurnal variation of PMF factors based on SP-AMS measurements, note that the O/C of HOA here is different with that in Luo et al. (2022) because of the mislabeling and corrected here.

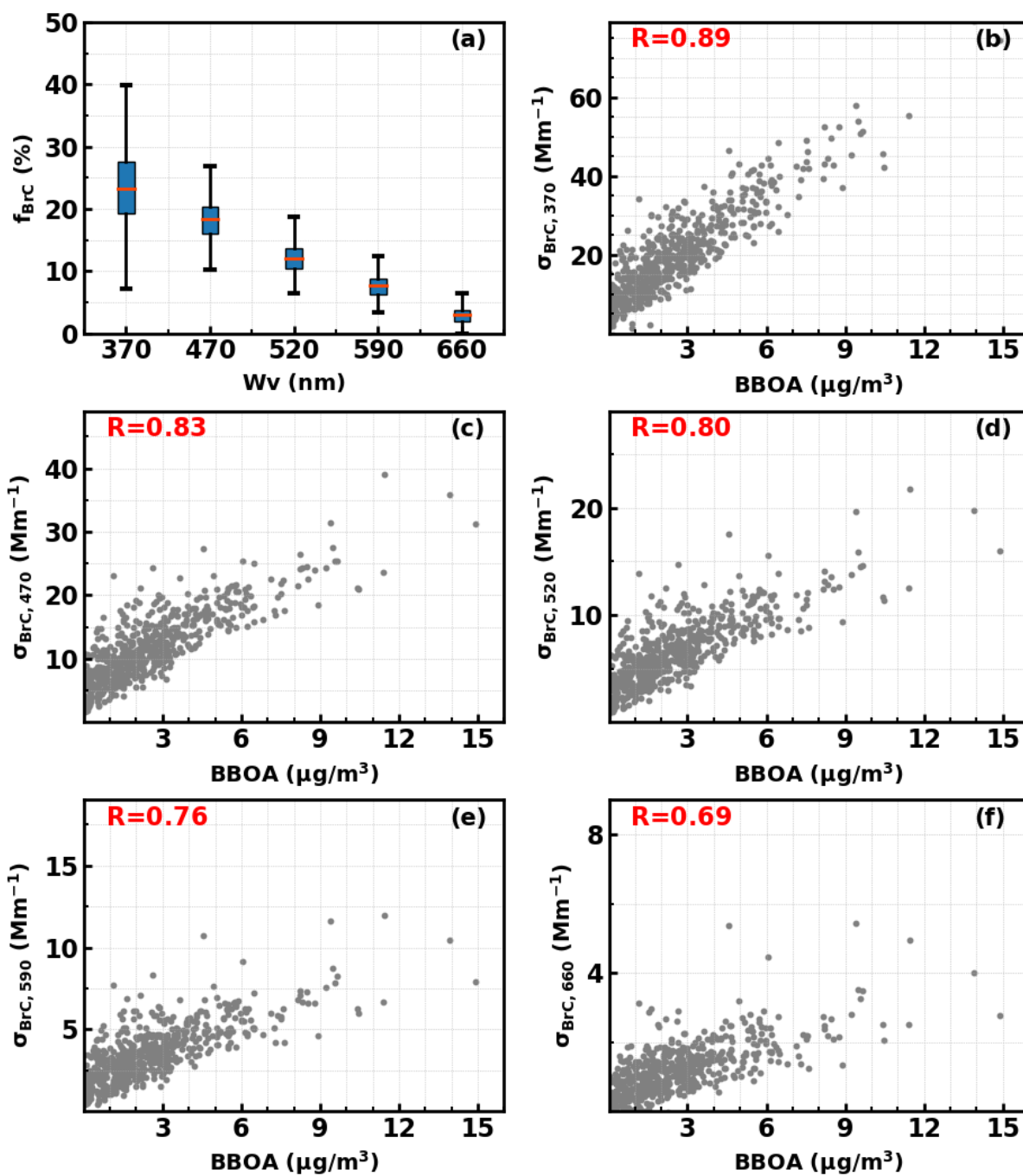


Figure S2. (a) Box-and-whisker plots of BrC absorption fractions at different wavelengths; (b-f) Correlations between BrC absorptions at 370 nm, 470 nm, 520 nm, 590 nm and 660 nm with BBOA.

52
53
54
55
56
57
58

59
60
61
62
63
64
65
66

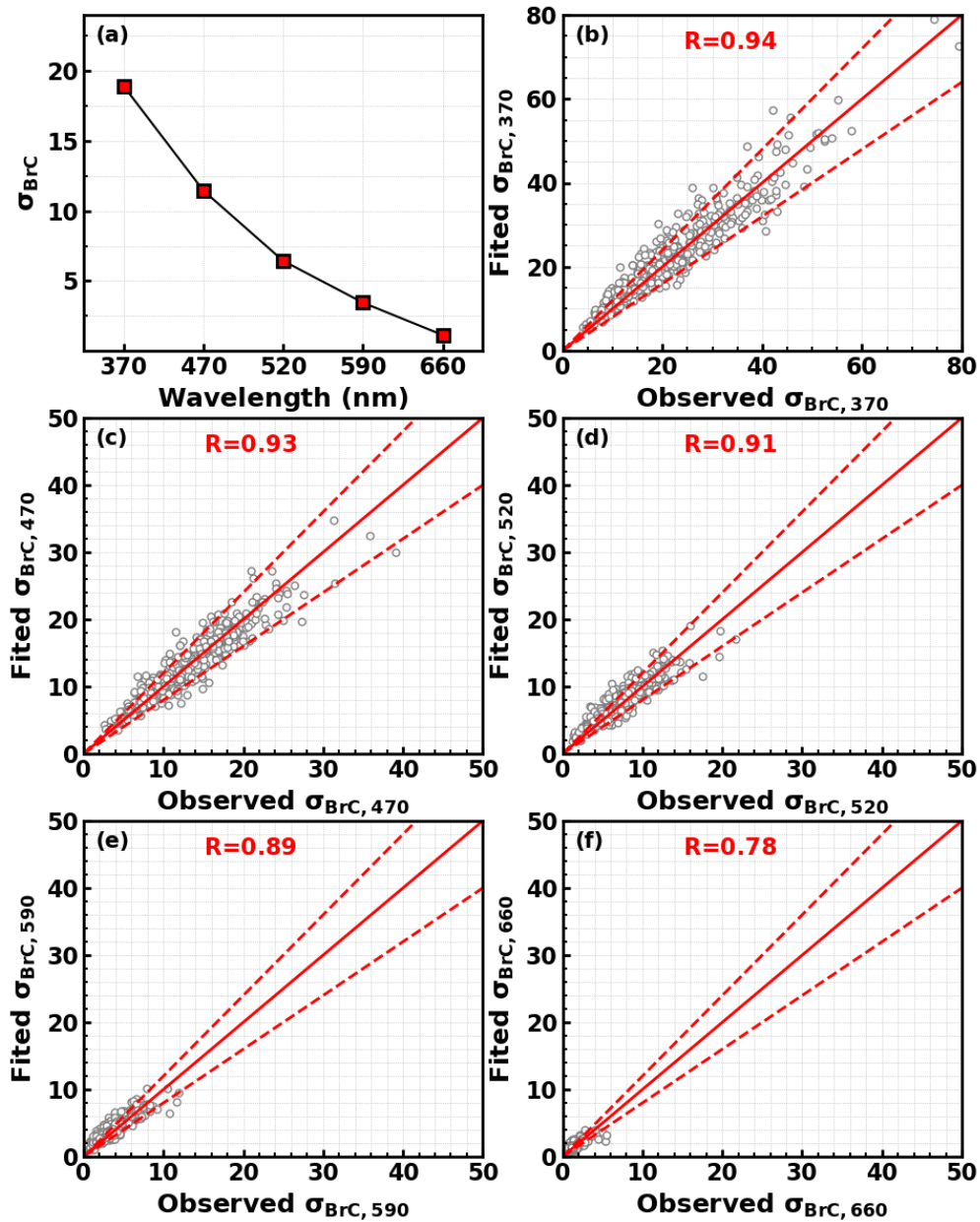


Figure S3. (a) Average BrC absorptions at different wavelengths, (b-f) Comparisons between predicted and observed BrC absorption values at wavelengths of 370 nm, 470 nm, 520 nm, 590 nm, and 660 nm using the multivariate linear regression method.

67

68
69
70
71
72

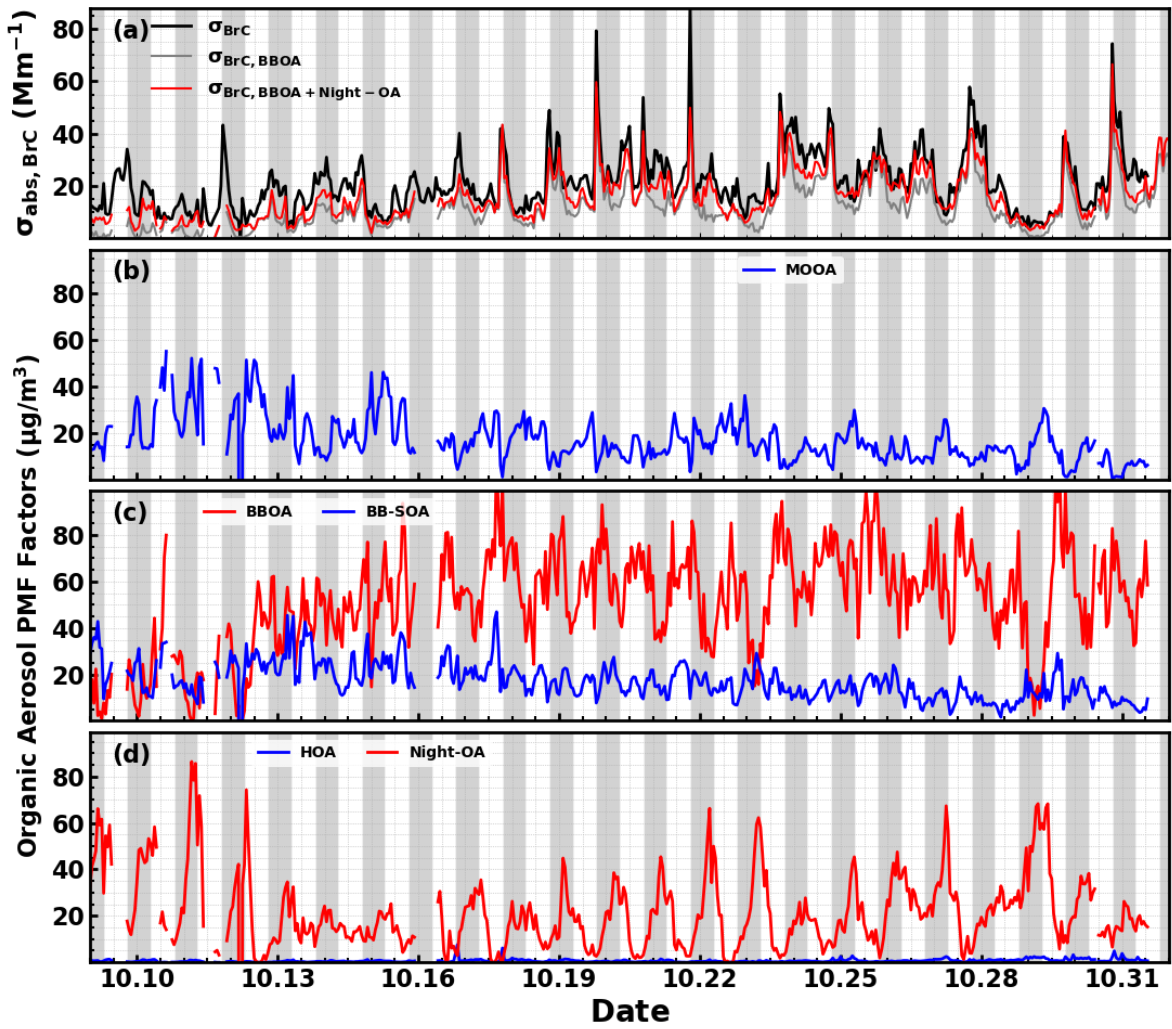


Figure S4. Timeseries of contributions of different OA factors to BrC absorption at 370 nm.

73
74
75
76
77
78
79
80
81
82
83
84

85
86
87
88
89
90

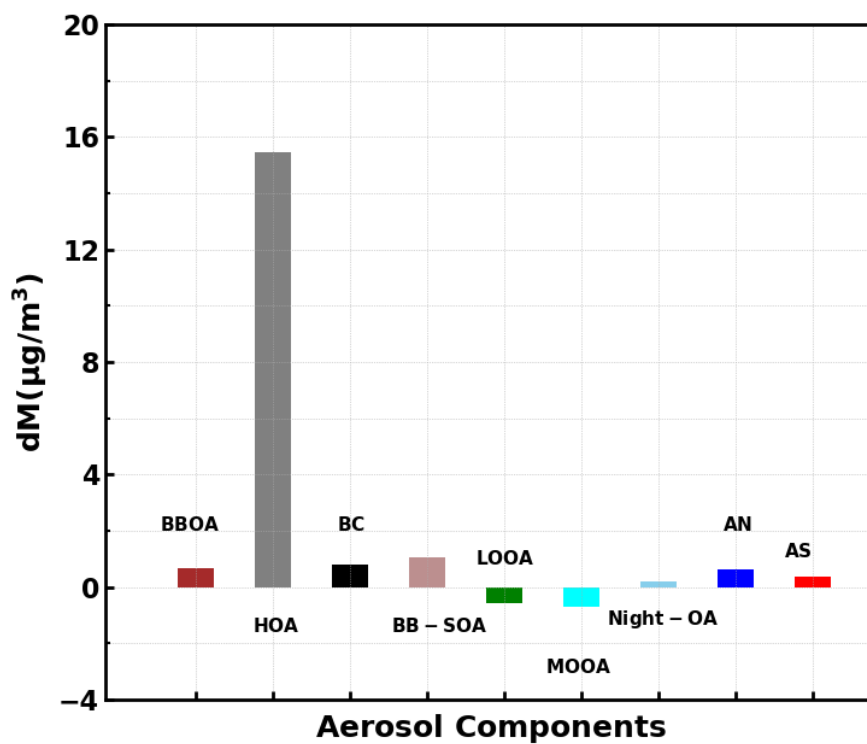


Figure S5. Average mass concentration changes of aerosol components for identified HOA increase cases, AN represents ammonium nitrate and AS represents ammonium sulfate.

91
92
93
94
95
96
97
98
99
100
101
102
103
104
105

106
107
108
109
110
111
112
113
114
115

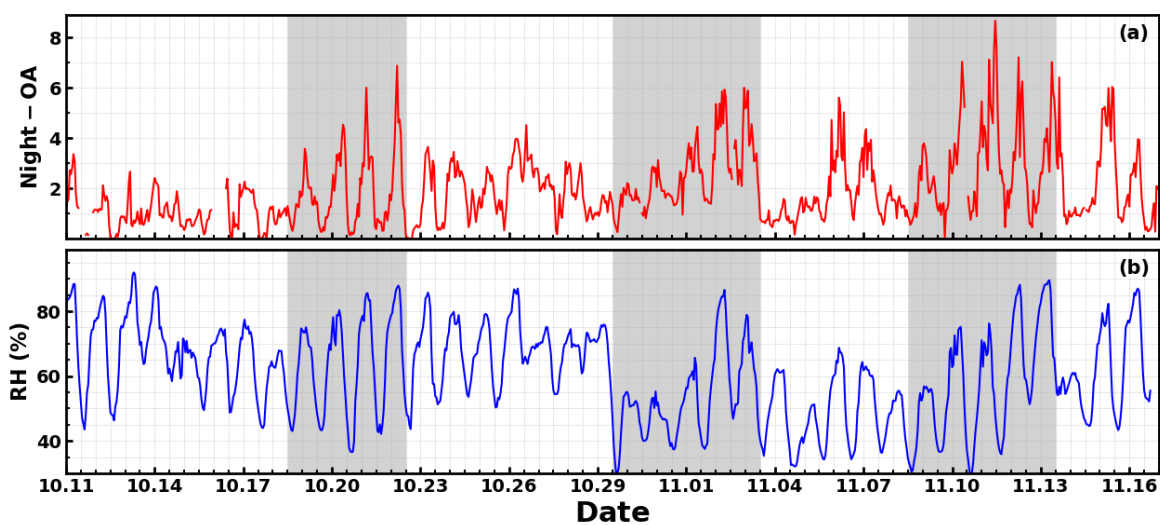


Figure S6. Timeseries of (a) Night-OA mass concentrations and (b) relative humidity (RH). Gray shading areas represent periods with remarkable Night-OA formations.

116
117
118
119
120
121
122
123
124
125
126
127
128
129
130
131
132
133

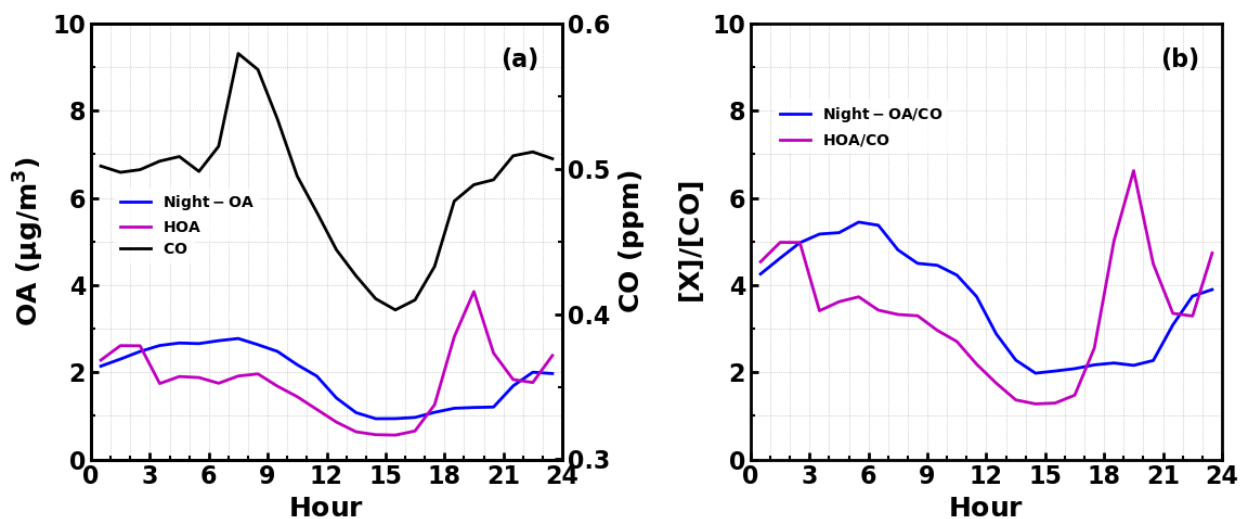


Figure S7. (a) Average diurnal variations of Night-OA, HOA and CO; (b) Average diurnal variations of [Night-OA]/[CO] and [HOA]/[CO]

135

136

137

138

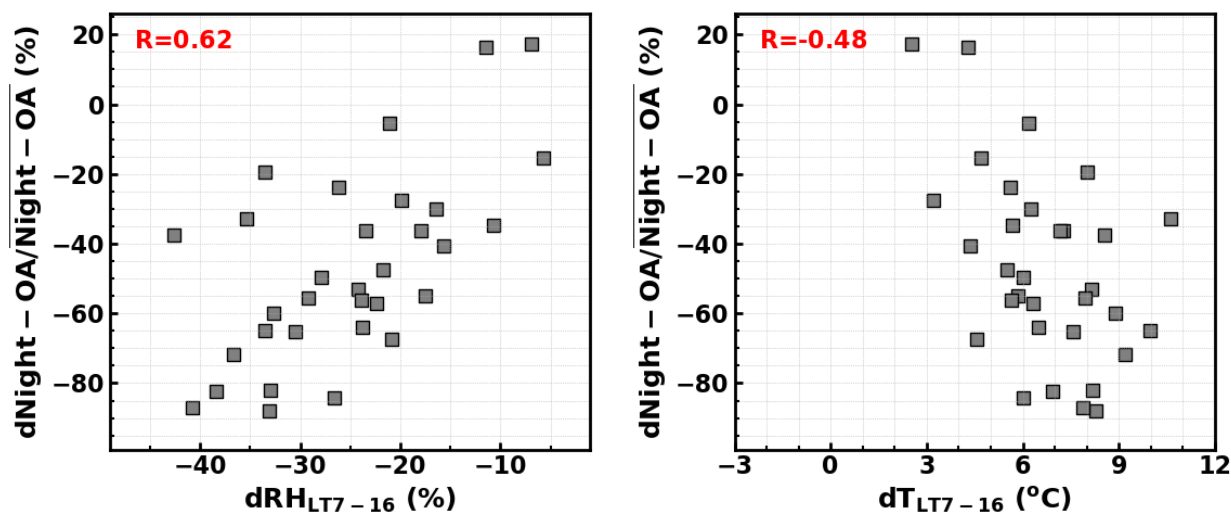


Figure S8. (a) Correlations between Night-OA decrease and RH changes from local time 07:00 in the morning to 16:00 in the afternoon; (b) Correlations between Night-OA decrease and air temperature (T) changes from local time 07:00 in the morning to 16:00 in the afternoon.

139

140

141

142

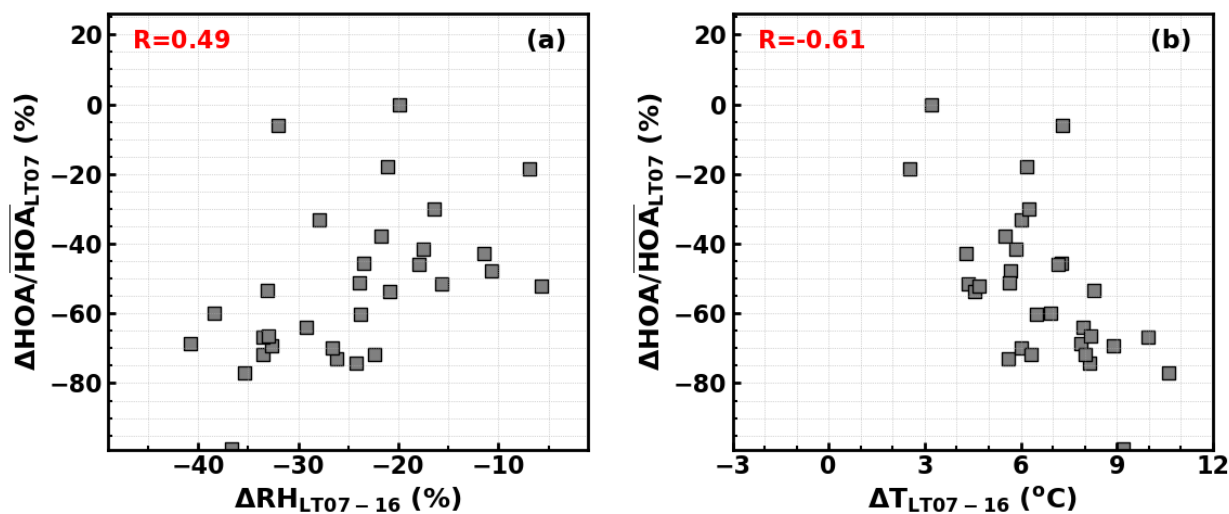


Figure S9. (a) Correlations between HOA decrease and RH changes from local time 07:00 in the morning to 16:00 in the afternoon; (b) Correlations between HOA decrease and air temperature (T) changes from local time 07:00 in the morning to 16:00 in the afternoon.

143
144
145
146
147

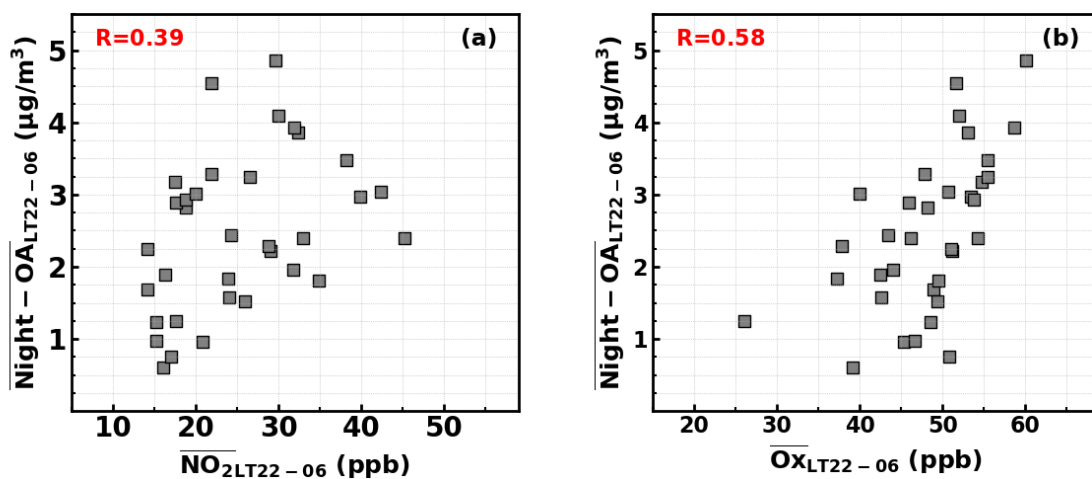


Figure S10. (a) Correlations between average Night-OA mass concentration (local time 22:00 to 06:00 of next morning) and corresponding average NO_2 concentration; (b) Correlations between average Night-OA mass concentration (local time 22:00 to 06:00 of next morning) and corresponding average Ox ($\text{NO}_2 + \text{O}_3$) concentration.

148
149
150

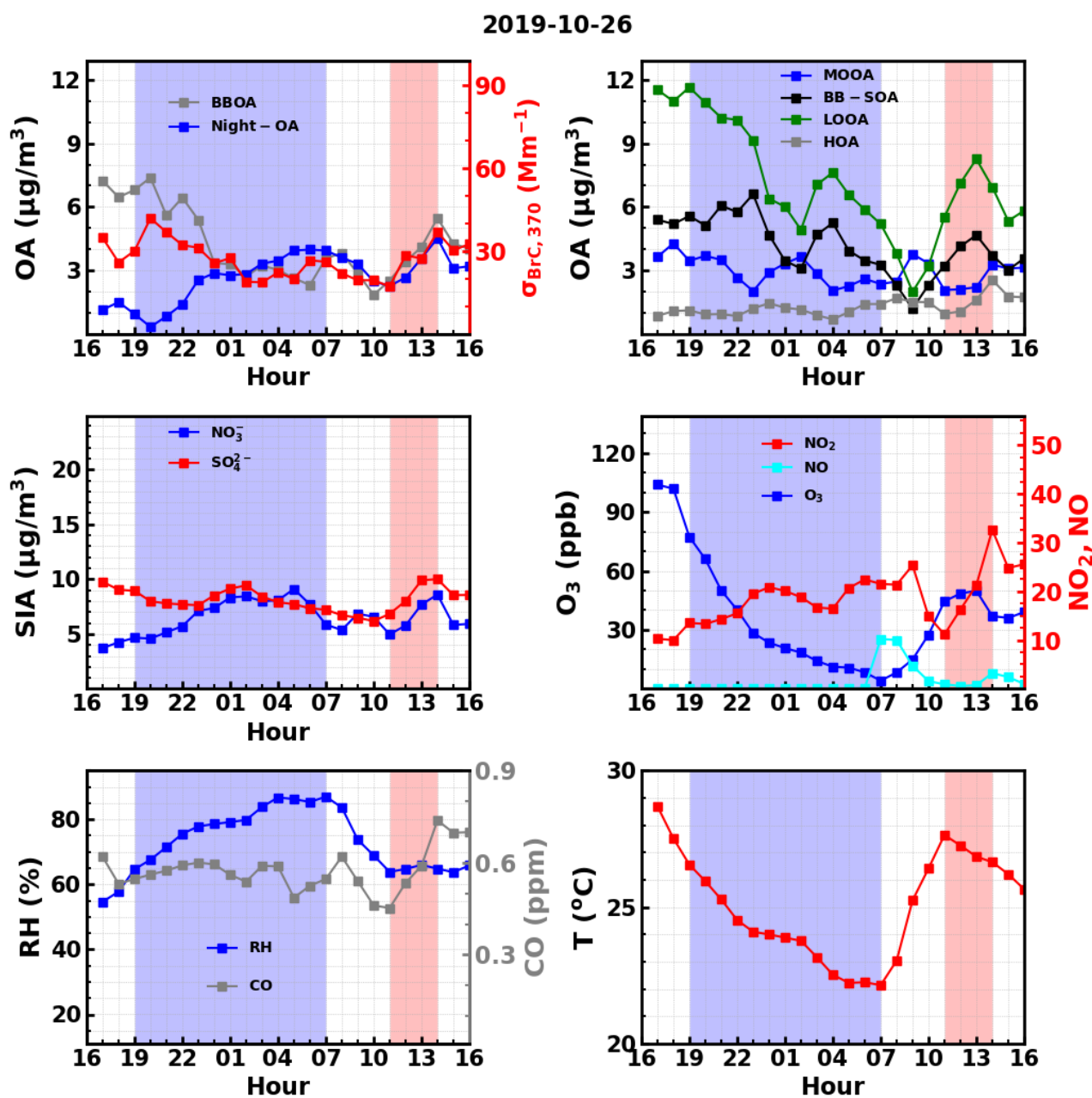


Figure S11. Evolution of aerosol chemical compositions, NO_2 , O_3 , NO CO, and meteorological parameters such as RH and T from local time 16:00 of 25th 10, 2019 to 16:00 of 26th 10, 2019, blue shading areas represent nighttime and pink shading areas corresponding to periods with obvious daytime Night-OA increase.

152

153

154

155

156

157

2019-11-11

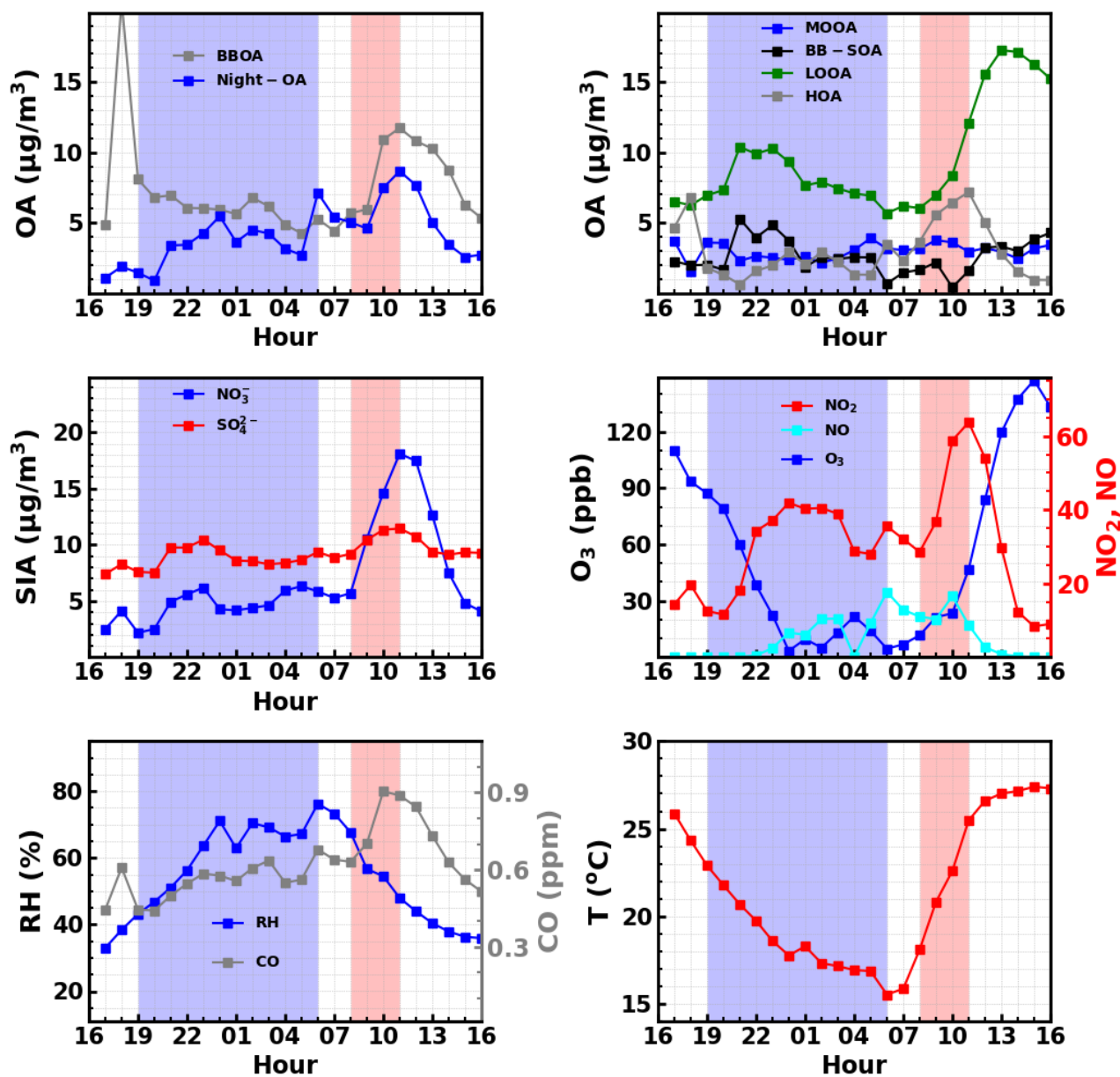


Figure S12. Evolution of aerosol chemical compositions, NO_2 , O_3 , NO , CO , and metrological parameters such as RH and T from local time 16:00 of 10th 11, 2019 to 16:00 of 11th 11, 2019, blue shading areas represent nighttime and pink shading areas corresponding to periods with obvious daytime Night-OA increase.

159

160

161

162

163

164

165

166 **References:**
167 Kuang, Y., Zhao, C. S., Zhao, G., Tao, J. C., Xu, W., Ma, N., and Bian, Y. X.: A novel method for calculating ambient aerosol
168 liquid water content based on measurements of a humidified nephelometer system, *Atmospheric Measurement*
169 *Techniques*, 11, 2967-2982, 10.5194/amt-11-2967-2018, 2018.
170 Kuang, Y., Huang, S., Xue, B., Luo, B., Song, Q., Chen, W., Hu, W., Li, W., Zhao, P., Cai, M., Peng, Y., Qi, J., Li, T., Chen, D., Yue,
171 D., Yuan, B., and Shao, M.: Contrasting effects of secondary organic aerosol formations on organic aerosol hygroscopicity,
172 *Atmos. Chem. Phys. Discuss.*, 2021, 1-27, 10.5194/acp-2021-3, 2021.
173 Luo, B., Kuang, Y., Huang, S., Song, Q., Hu, W., Li, W., Peng, Y., Chen, D., Yue, D., Yuan, B., and Shao, M.: Parameterizations
174 of size distribution and refractive index of biomass burning organic aerosol with black carbon content, *Atmos. Chem. Phys.*,
175 22, 12401-12415, 10.5194/acp-22-12401-2022, 2022.
176